



Computer-Aided Detection and Classification of Masses in Digitized Mammograms

Mohammed Jahirul Islam

November 20, 2009

Presentation Outline

- **Introduction**
- **Breast Cancer Statistics**
- **Motivation, Objectives**
- **Principal Stages of Breast Cancer Detection**
- **Literature Survey**
 - Image Enhancement
 - Image Segmentation
 - Feature Extraction and Selection
 - Classification
- **Proposed Method of Computer-Aided Diagnosis (CAD) System**
- **Simulation Results and Performance Evaluation**
- **Conclusions**

Introduction




- Breast cancer continues to be a public health problem in the world.
- Breast cancer is the second leading cause of death by disease in Canada for women, after lung cancer.

Breast Cancer Statistics

- **Breast Cancer Statistics in 2009***
 - an estimated 22,700 Canadian women will be diagnosed with breast cancer and 5,400 will die from it.
 - An estimated 170 men will be diagnosed with breast cancer and 50 will die of it.
 - 1 in 9 women (11%) is expected to develop breast cancer during her lifetime (by age 90) and one in 28 will die from it.
- **Early detection of breast cancer, allowing treatment at an earlier stage, can significantly reduce breast cancer mortality.**

**Source: Canadian Cancer Society / National Cancer Institute of Canada; Canadian Cancer Statistics 2009, Toronto, Canada*

Motivation

- Mammography has been one of the most reliable methods for early detection of breast carcinomas.
 - X-ray mammography is currently considered the “gold standard” for breast cancer diagnosis.
 - However, It is difficult for radiologists to provide both accurate and uniform evaluation for the enormous mammograms.
 - The estimated sensitivity of radiologists in breast cancer screening is only about 75% [80]
- 
- **Computer-aided diagnosis (CAD) system can be used as a second opinion to aid the radiologist by indicating the locations of suspicious abnormalities in mammograms**

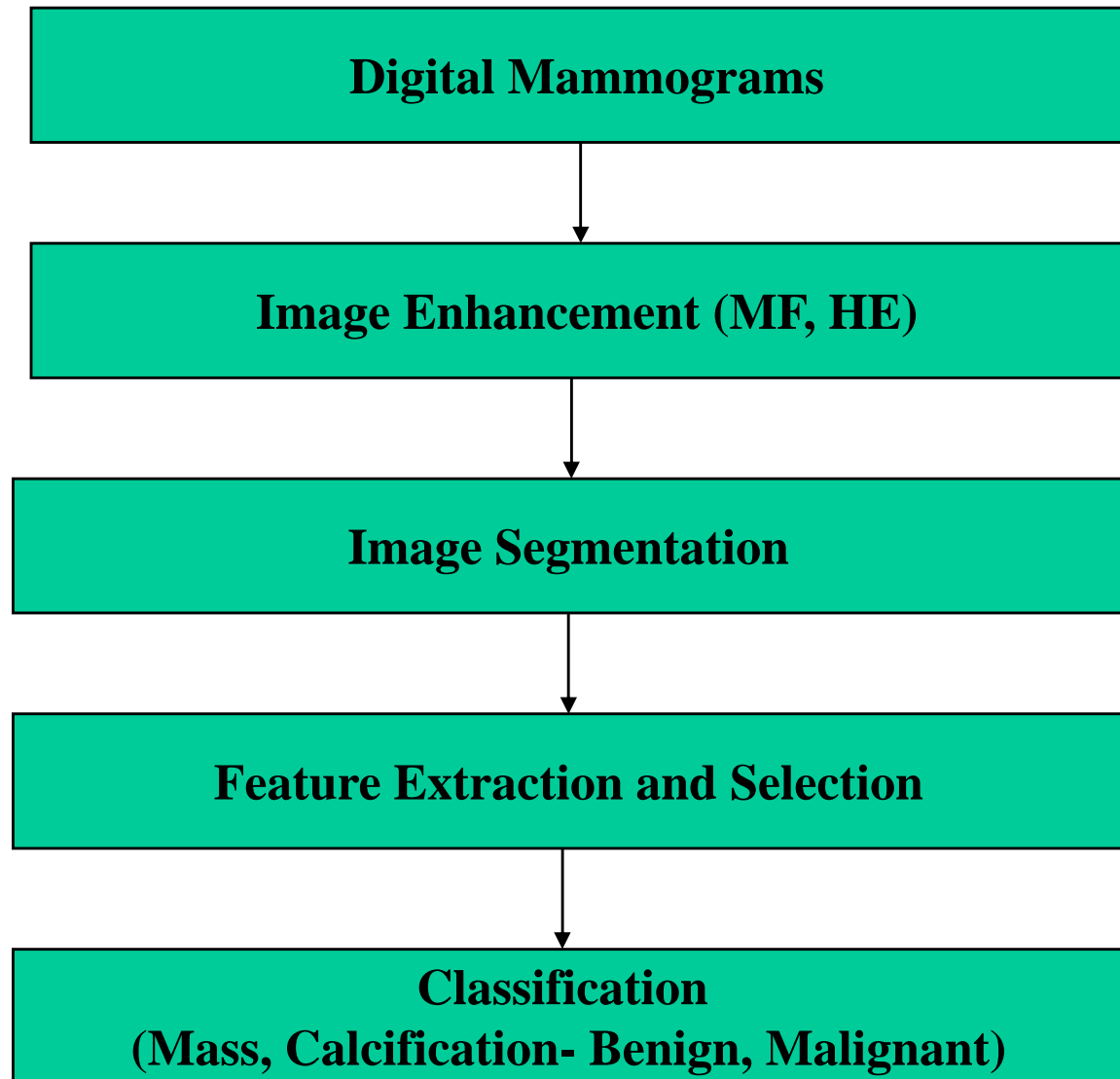
Objectives

- **Develop a CAD system for breast cancer diagnosis and detection based on automated segmentation of masses in mammograms.**
- The ultimate diagnosis of all types of breast disease depends on a biopsy. In most cases the decision for a biopsy is based on mammography findings.
- Biopsy results indicate that 65-90% of suspected cancer detected by mammography turned out to be benign [81]
- **The objective of the automated methods for classifications is to provide a tentative diagnosis (the final decision is produced by human expert) of individual masses, based on their physical attributes.**

Challenges in Breast Cancer Detection

- Microcalcifications and Masses are two important early signs of breast cancer.
- Masses are often indistinguishable from the surrounding parenchyma because their features can be obscured or similar to the normal inhomogeneous breast tissues.
- This makes the automatic mass detection and classification challenging

Principal Stages of Breast Cancer Detection



Sample Mammograms



Image 1: Normal Breast



Image 2: Cancerous Breast

Survey Over Image Enhancement Techniques

- **Global approach (HE) [33-36]**
 - Reassign the intensity values of pixels to make the new distribution of the intensities uniform to the utmost extent
 - Effective in enhancing the entire image with low contrast
 - Can not enhance the textural information.
 - Working only for the images having one object
- **Local Approach [33, 37-38]**
 - Feature-based or using non-linear mapping locally (Median filtering)
 - Effective in local texture enhancement
 - Can not enhance the entire image well

Survey Over Image Segmentation Techniques

- **Image Segmentation-** Recognize homogeneous regions within an image as distinct and belonging to different objects.
- The segmentation process can be based on finding the maximum homogeneity in grey levels within the regions identified. The segmentation doesn't perform well if the grey levels of different objects are quite similar [**M.A. Sid-Ahmed**]
- **Global Thresholding [39, 40, 43]**
 - Based on global information, such as histogram of the mammograms
 - Widely used, easy to implement
 - Not good for identifying ROIs
 - FNs and FPs may be too high

Survey Over Image Segmentation Techniques

- **Local Thresholding [7, 41, 42, 44]**
 - Thresholding value is determined locally
 - It can refine the results of global thresholding, and is better for mass detection than global thresholding
 - It can not accurately separate the pixels into suitable sets. It is often used as an initialization of other algorithms
- **Edge Detection [35, 43, 48-53]**
 - Traditional method for image segmentation and it detects the discontinuity in mammograms
- **Template Matching [54-59]**
 - Segments possible masses from the background using prototypes
 - Easy to implement; if the prototypes are appropriate, it can provide good results
 - It depends on the prior information of the masses, it may result high number of false positives

Survey Over Image Segmentation Techniques

- **Region Growing [44-47]**
 - Finds a set of seed pixels first, then grow iteratively and aggregate with the pixels that have similar properties
- **Bilateral Image Subtraction [60-66]**
 - It is based on the normal symmetry between the left and right breast
 - Easy to implement, and the difference between the left and right mammogram images can be identified as suspicious regions
 - It is difficult to register the left and right breast correctly
- **Fuzzy Techniques [67-71]**
 - The fuzzy techniques including fuzzy thresholding and fuzzy region growing; it can handle the unclear boundary between normal tissue and tumors
 - It is not easy to determine suitable membership functions and rules

Survey Over Features Extraction and Selection

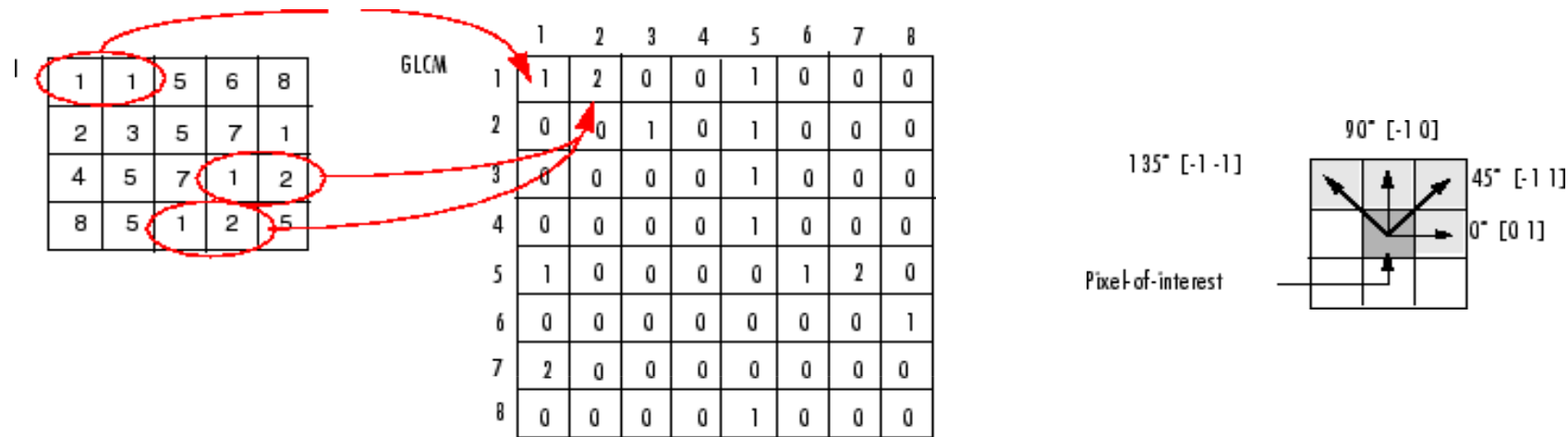
- Features extraction and selection is a key step in mass detection and classification
- Features are calculated from the region of interest (ROI) characteristics such as size, shape, density and smoothness etc. [72]
- Feature space is very large and complex due to wide diversity of the normal tissues and the variety of the abnormalities.
- Feature space can be divided into 3 sub-spaces [73]
 - Intensity features
 - Shape features
 - Texture features

Haralick Texture Features- GLCM

- The basis for Haralick features [79] is the Gray-Level Co-occurrence Matrix (GLCM) or Spatial Gray Level Dependence (SGLD) Matrix
- This matrix is square with dimension N_g , where N_g is the number of gray levels in the image.
- Element $[i,j]$ of the matrix is generated by counting the number of times a pixel with value i is adjacent to a pixel with value j and then dividing the entire matrix by the total number of such comparisons made.
- Each entry is therefore considered to be the probability that a pixel with value i will be found adjacent to a pixel of value j .

$$\mathbf{G} = \begin{bmatrix} p(1,1) & p(1,2) & \cdots & p(1, N_g) \\ p(2,1) & p(2,2) & \cdots & p(2, N_g) \\ \vdots & \vdots & \ddots & \vdots \\ p(N_g, 1) & p(N_g, 2) & \cdots & p(N_g, N_g) \end{bmatrix}$$

Example of GLCM



- Adjacency can be defined to occur in four directions in a 2D, square pixel image (horizontal, vertical, left and right diagonals, four such matrices can be calculated).
- Rotation invariance is a primary criterion for any features used with these images, a kind of invariance was achieved for each of these statistics by averaging them over the four directional co-occurrence matrices.

Haralick Texture Features (1-6)

Angular Second Moment

$$\sum_i \sum_j p(i, j)^2$$

Contrast

$$\sum_{n=0}^{N_g-1} n^2 \left\{ \sum_{i=1}^{N_g} \sum_{j=1}^{N_g} p(i, j) \right\}, |i - j| = n$$

Correlation

$$\frac{\sum_i \sum_j (ij) p(i, j) - \mu_x \mu_y}{\sigma_x \sigma_y}$$

where μ_x , μ_y , σ_x , and σ_y are the means and std. deviations of p_x and p_y , the partial probability density functions

Sum of Squares: Variance

$$\sum_i \sum_j (i - \mu)^2 p(i, j)$$

Inverse Difference Moment

$$\sum_i \sum_j \frac{1}{1 + (i - j)^2} p(i, j)$$

Sum Average

$$\sum_{i=2}^{2N_g} i p_{x+y}(i)$$

where x and y are the coordinates (row and column) of an entry in the co-occurrence matrix, and $p_{x+y}(i)$ is the probability of co-occurrence matrix coordinates summing to $x + y$

Haralick Texture Features (7-13)

Sum Variance	$\sum_{i=2}^{2N_g} (i - f_s)^2 p_{x+y}(i)$
Sum Entropy	$-\sum_{i=2}^{2N_g} p_{x+y}(i) \log\{p_{x+y}(i)\} = f_s$
Entropy	$-\sum_i \sum_j p(i, j) \log(p(i, j))$
Difference Variance	$\sum_{i=0}^{N_g-1} i^2 p_{x-y}(i)$
Difference Entropy	$-\sum_{i=0}^{N_g-1} p_{x-y}(i) \log\{p_{x-y}(i)\}$
Info. Measure of Correlation 1	$\frac{HXY - HXY1}{\max\{HX, HY\}}$
Info. Measure of Correlation 2	$(1 - \exp[-2(HXY2 - HXY)])^{\frac{1}{2}}$ where $HXY = -\sum_i \sum_j p(i, j) \log(p(i, j))$, HX , HY are the entropies of p_x and p_y , $HXY1 =$ $-\sum_i \sum_j p(i, j) \log\{p_x(i)p_y(j)\}$ $HXY2 =$ $-\sum_i \sum_j p_x(i)p_y(j) \log\{p_x(i)p_y(j)\}$
Max. Correlation Coeff.	Square root of the second largest eigenvalue of \mathbf{Q} where $\mathbf{Q}(i, j) = \sum_k \frac{p(i, k)p(j, k)}{p_x(i)p_y(k)}$

Survey Over Classification Techniques

- **Linear Discriminant Analysis (LDA) [74, 75]**
 - Traditional method for classification
 - Construct decision boundaries by optimizing certain criteria to classify cases into one of mutually exclusive classes
 - High performance for linear separable problems, poor for non linear separable data
- **Artificial Neural Network [76-78]**
 - Construct non-linear mapping function as a decision boundaries.
 - Two kinds: 3 layers back propagation of NN and Radial Basis Function (RBF) network
 - Robust, no rule or explicit expression is needed, widely applicable
 - No common rule to determine to size of the ANNs, long training time, over training.

Image Database

- **Mini-MIAS**- The Mammographic Image Analysis Society [Suckling et al., 1994]
 - An organization of UK research group.
 - Films taken from UK National Breast Screening Programme
 - Includes radiologist's "truth"-markings on the locations of any abnormalities that may be present
 - Available Online at the Pilot European Image Processing Archive (PEIPA) at the University of Essex
 - <http://peipa.essex.ac.uk/info/mias.html>
- Total Patients: 161
- Total Image: 322 (Left and Right Breast)
 - Images are digitized at a resolution of 1024x1024 and 8 bit gray level scale
 - Each image includes the location of abnormality, its radius, breast position, type of breast and tumor type

Proposed Method- ROI Extraction

- **X-ray label Removal- Global ROI**
 - Global thresholding (Otsu)
 - Connected component labeling
 - Calculate no. of pixels in each region
 - Pick the biggest region- Extracted breast region
- **Pectoral Muscle Removal**
 - Mass and pectoral region may have similar texture characteristics, causing a high number of FPs when detecting suspicious masses.
 - It is a higher density than the surrounding tissue
 - Automated region growing
- **Mass Extraction**
 - Mass is slightly brighter than its surrounding areas, produces a sharp peak of unusual gray level intensity pixels
 - Peak analysis of the histogram
 - Extract significant peak regions- **ROIs**

Proposed Method- Image Enhancement

- **Removal of Noise Effects**

- Median filtering- very powerful in removing noise from 2D signals without blurring edges
- Noise pixels generally have little correlation with mass pixels, median filter can smooth out these pixels so as to reduce their effects.

$$I_2(x, y) = \text{median} \{I_1(x, y)\} = \text{median} \left\{ \sum_{i=-1}^1 \sum_{j=-1}^1 I_1(x+i, y+j) \right\}$$

- **Contrast Enhancement**

$$I_{en}(i, j) = \left(\frac{I(i, j)}{I_{\max}} \right)^k * I_{\max}$$

$$k = 2, 3, 4, \dots$$

Proposed Method- Image Segmentation

- **Automatic Seeded Region Growing using Haralick texture features**
 - Divide enhanced ROI into $R \times R$ non-overlapping blocks
 - If block is too small, the difference of the mass textures from normal textures can not be well characterized.
 - If it is too large, the result may be too coarse
 - Calculate the Haralick texture features from Spatial Gray Level Dependence Matrix (SGLD) of each block
 - Select the significant features that can easily discriminate mass and non mass region.
 - Select the blocks that contains mass based on the features

Proposed Method- Image Segmentation (Cont'd)

- Maximum gray level of that block is the seed point
- Region growing starts from that point and then grow iteratively and aggregate with the pixels that have similar properties
- Approximate the segmented mass to a circle
- Estimate the radius of the circle and compare it with the ground-truth data
- This comparison will provide the results how close the segmented mass to the ground-truth mass determined by the expert radiologists.
- Extract the mass region from the original image that is used as an input for classification

Proposed Method- Classification (Benign or Malignant)

- **Classifier:** Artificial Neural Network
- **Input:** 7 texture features
- **Output:** Benign (0) or Malignant (1)

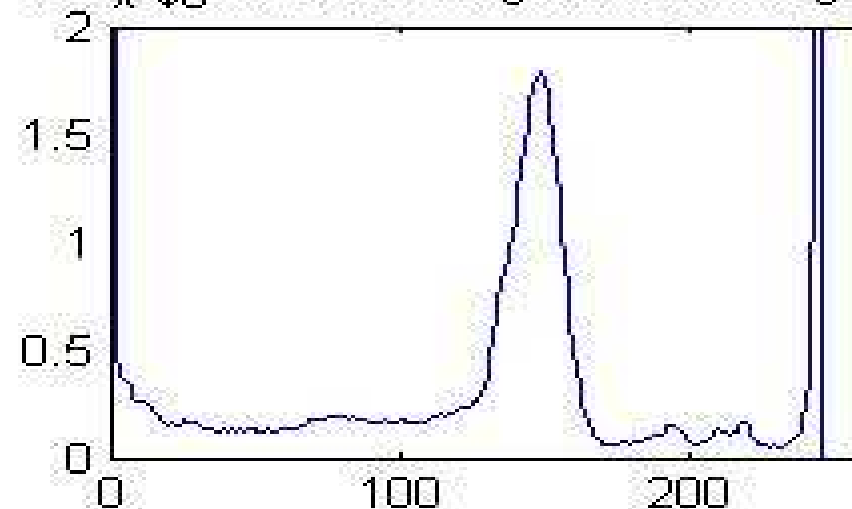
1. Mean	$\mu_{ij} = \frac{1}{(2n+1)^2} \sum_{x=i-n}^{i+n} \sum_{y=j-n}^{j+n} p(x, y)$	5. Skewness	$S_{ij} = \frac{1}{(2n+1)^2} \sum_{x=i-n}^{i+n} \sum_{y=j-n}^{j+n} \left[\frac{p(i, j) - \mu_{ij}}{\sigma_{ij}} \right]^3$
2. Standard Deviation	$\sigma_{ij} = \frac{1}{(2n+1)} \sqrt{\sum_{x=i-n}^{i+n} \sum_{y=j-n}^{j+n} (p(x, y) - \mu_{ij})^2}$	6. Kurtosis	$k_{ij} = \left\{ \frac{1}{(2n+1)^2} \sum_{x=i-n}^{i+n} \sum_{y=j-n}^{j+n} \left[\frac{p(i, j) - \mu_{ij}}{\sigma_{ij}} \right]^4 \right\} - 3$
3. Smoothness	$R_{ij} = 1 - \frac{1}{1 + \sigma_{ij}^2}$	7. Uniformity	$U_{ij} = \sum_{k=0}^{L-1} \text{Pr}_k^2$
4. Entropy	$h_{ij} = - \sum_{k=0}^{L-1} \text{Pr}_k (\log_2 \text{Pr}_k)$		

Simulation Results- X-ray Label Removal

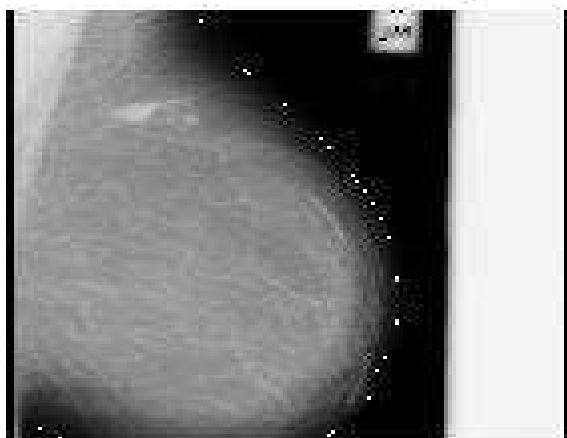
Original Mammogram mdb132.pgm



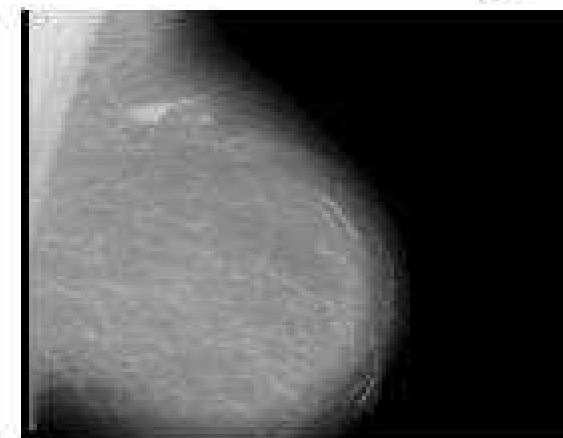
Histogram of the Original Mammogram



Outlined Breast Region

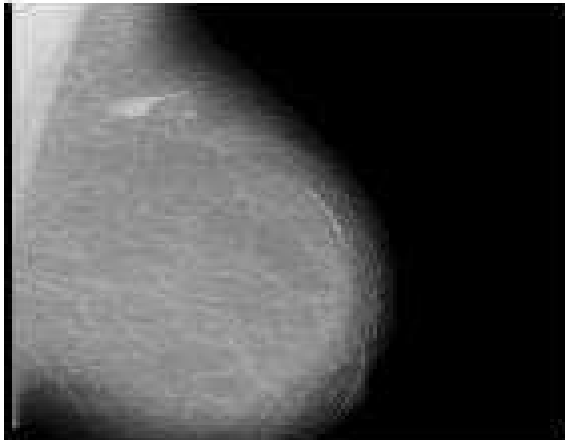


Extracted Breast Region



Simulation Results- Pectoral Muscle Removal

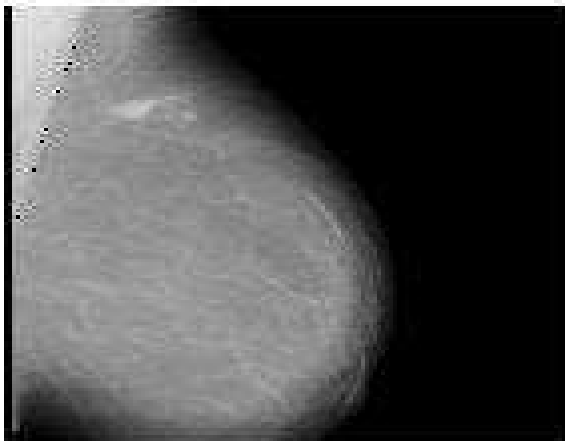
Breast Region



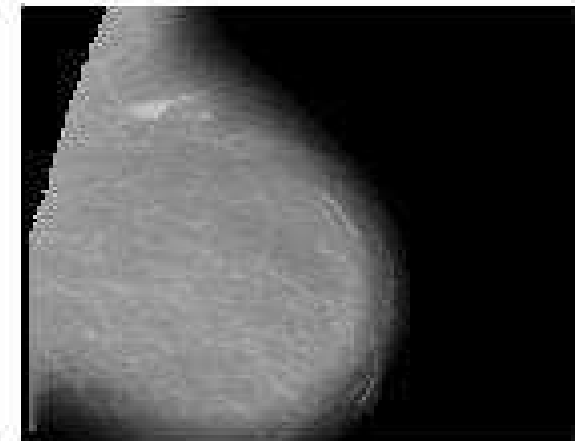
Pectoral Muscle



Outlined Pectoral Muscle

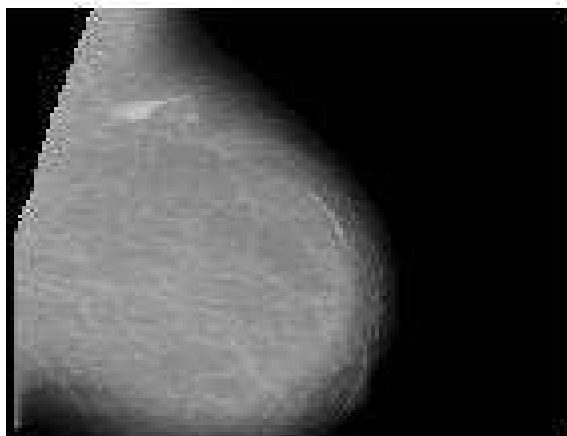


Pectoral Muscle suppressed Breast

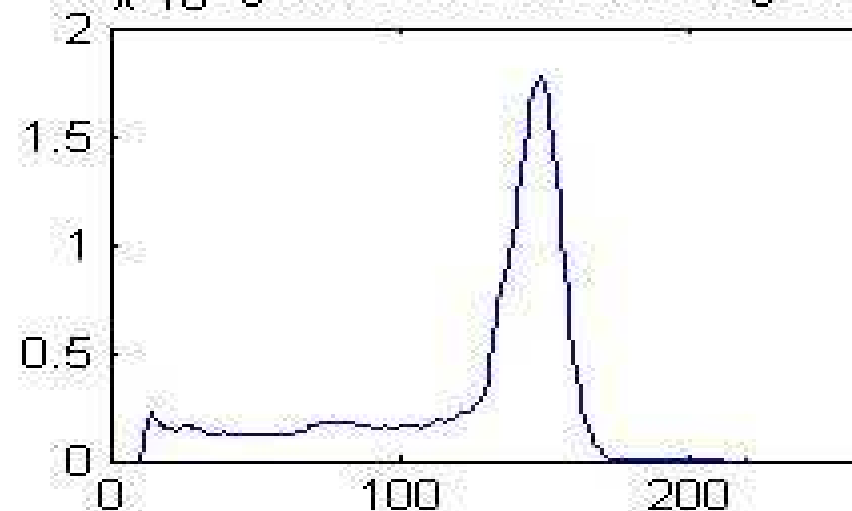


Simulation Results- ROI Extraction

Original Mammogram mdb132.pgm



Histogram of the Breast Region



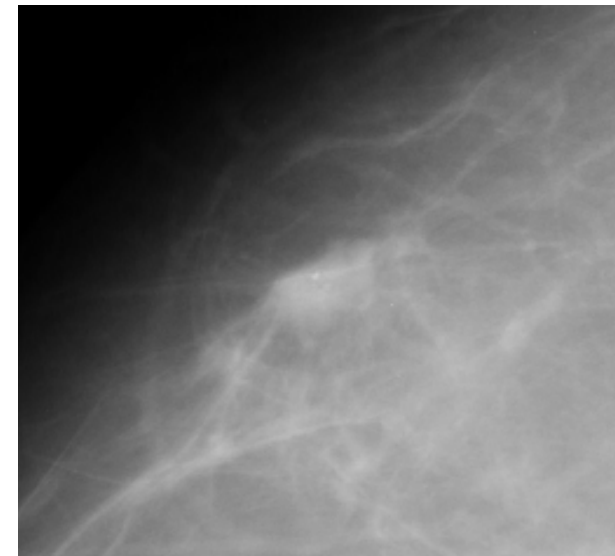
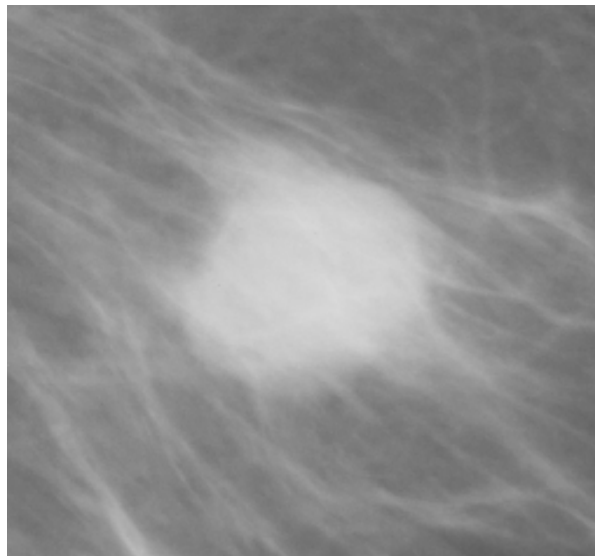
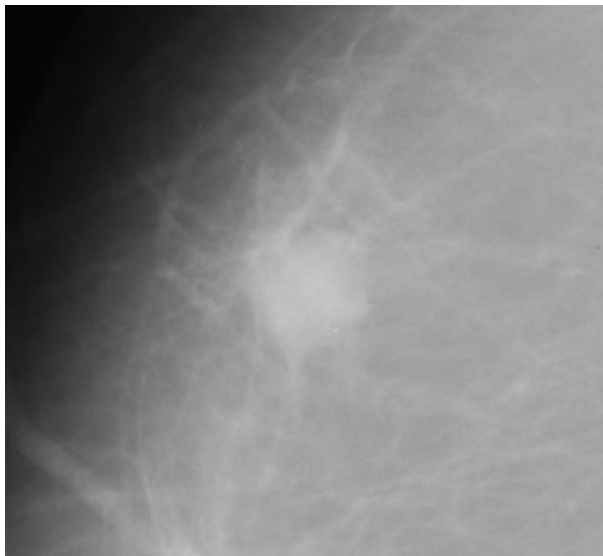
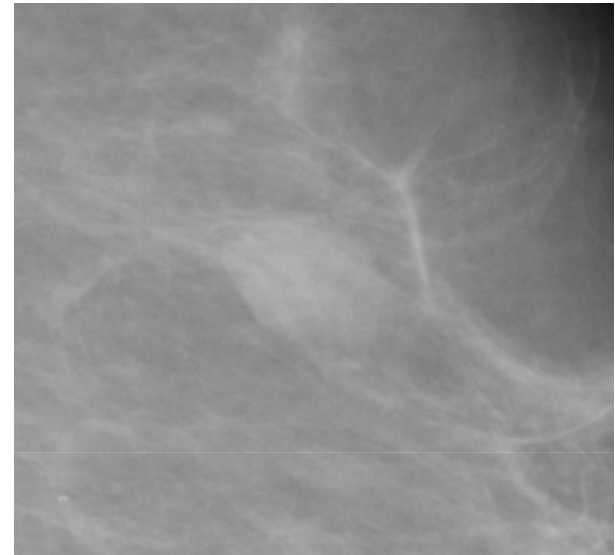
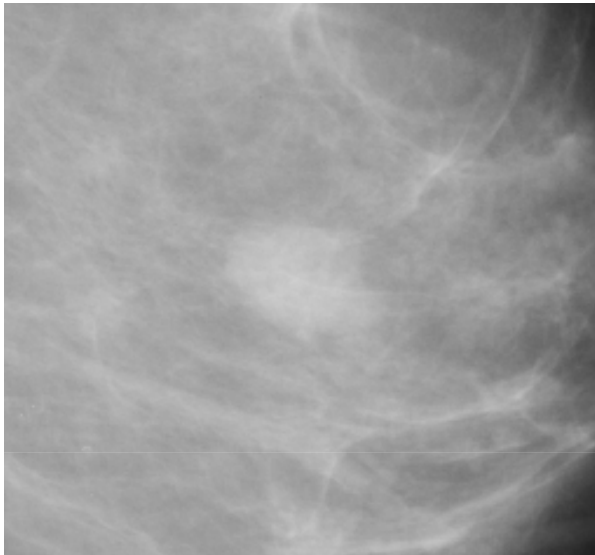
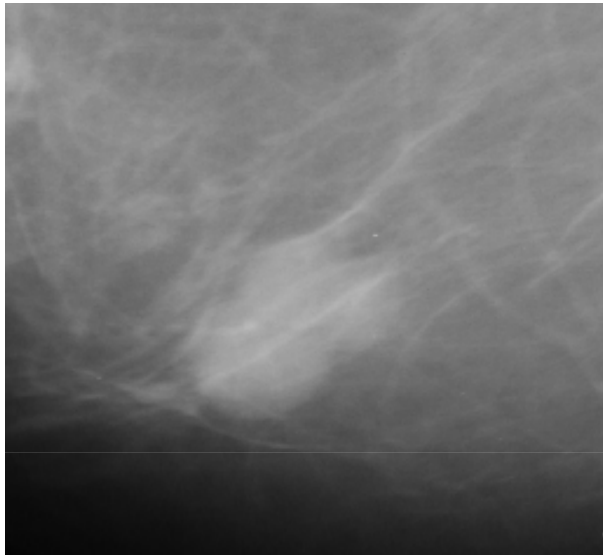
Extracted Significant Peak Region



Region of Interest



Sample ROIs



Simulation Results- Image Enhancement

Original Image



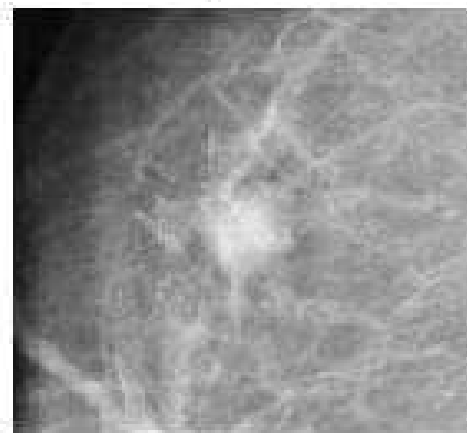
Histogram Equalization



Image Adjust



Adaptive HE

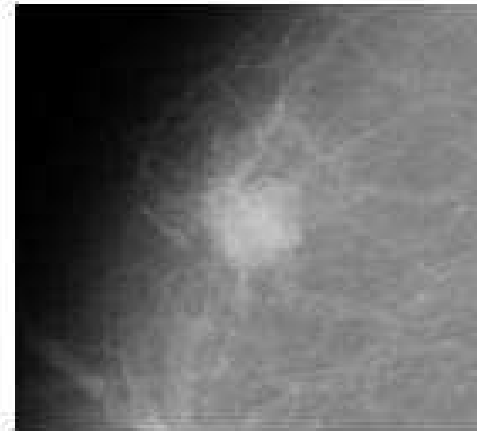


Simulation Results- Image Enhancement- Proposed

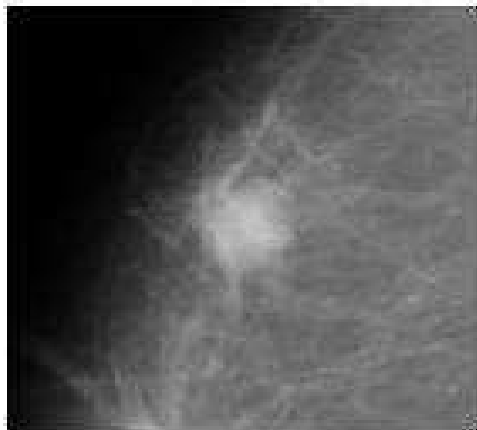
Original Image



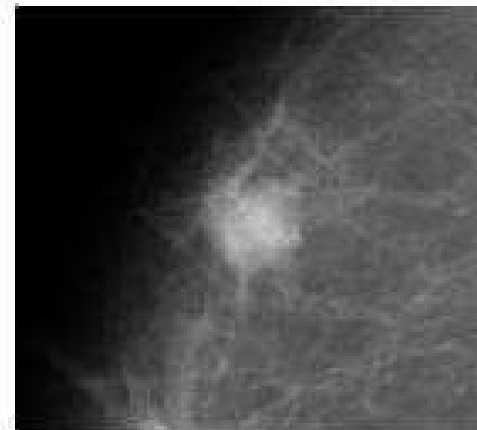
Enhanced Image-2



Enhanced Image-3



Enhanced Image-4



Simulation Results- Image Segmentation

Non-overlapped Enhanced Image

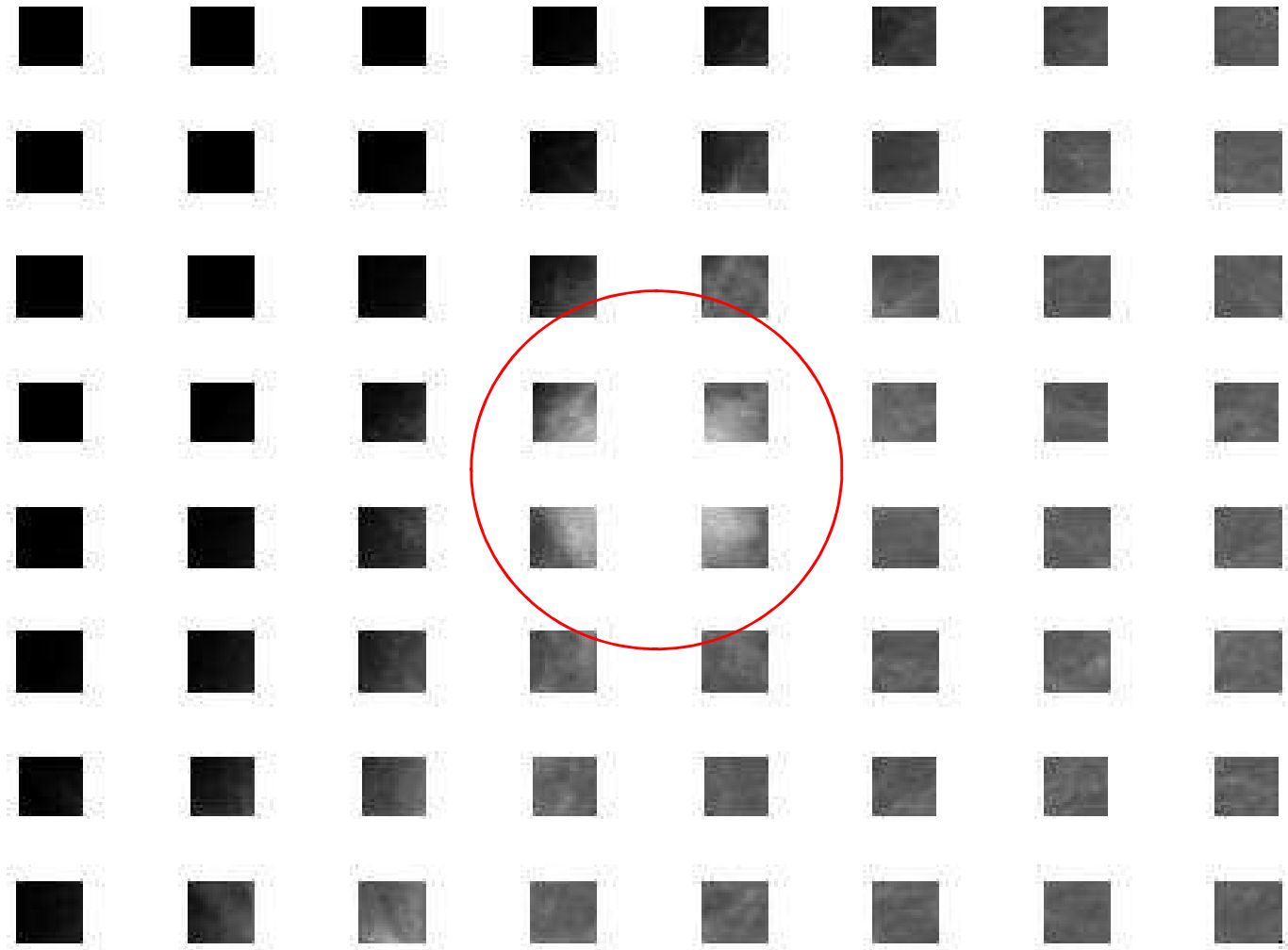


Image Segmentation- Haralick Features (1-4)

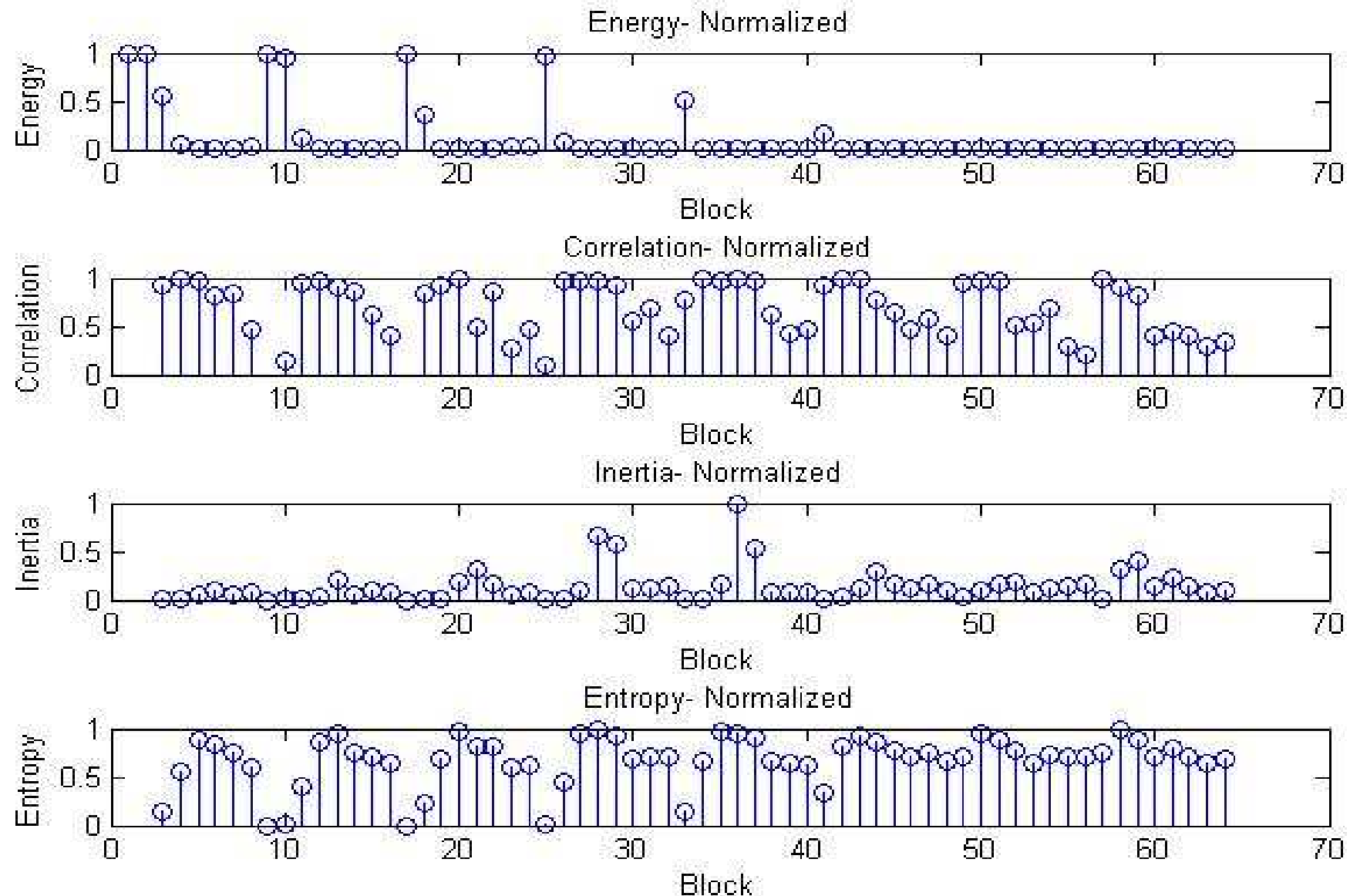


Image Segmentation- Haralick Features (5-8)

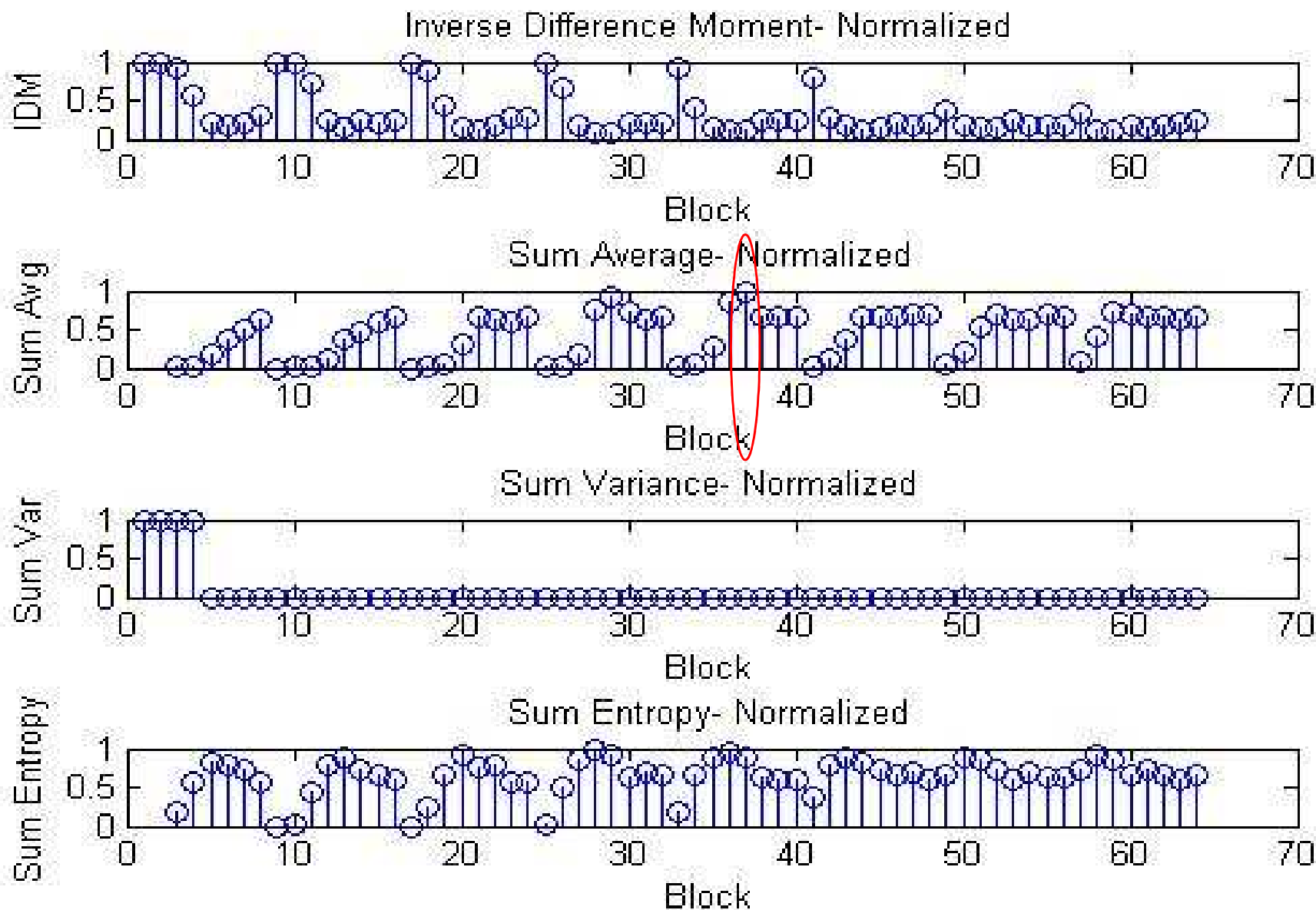


Image Segmentation- Haralick Features (9-13)

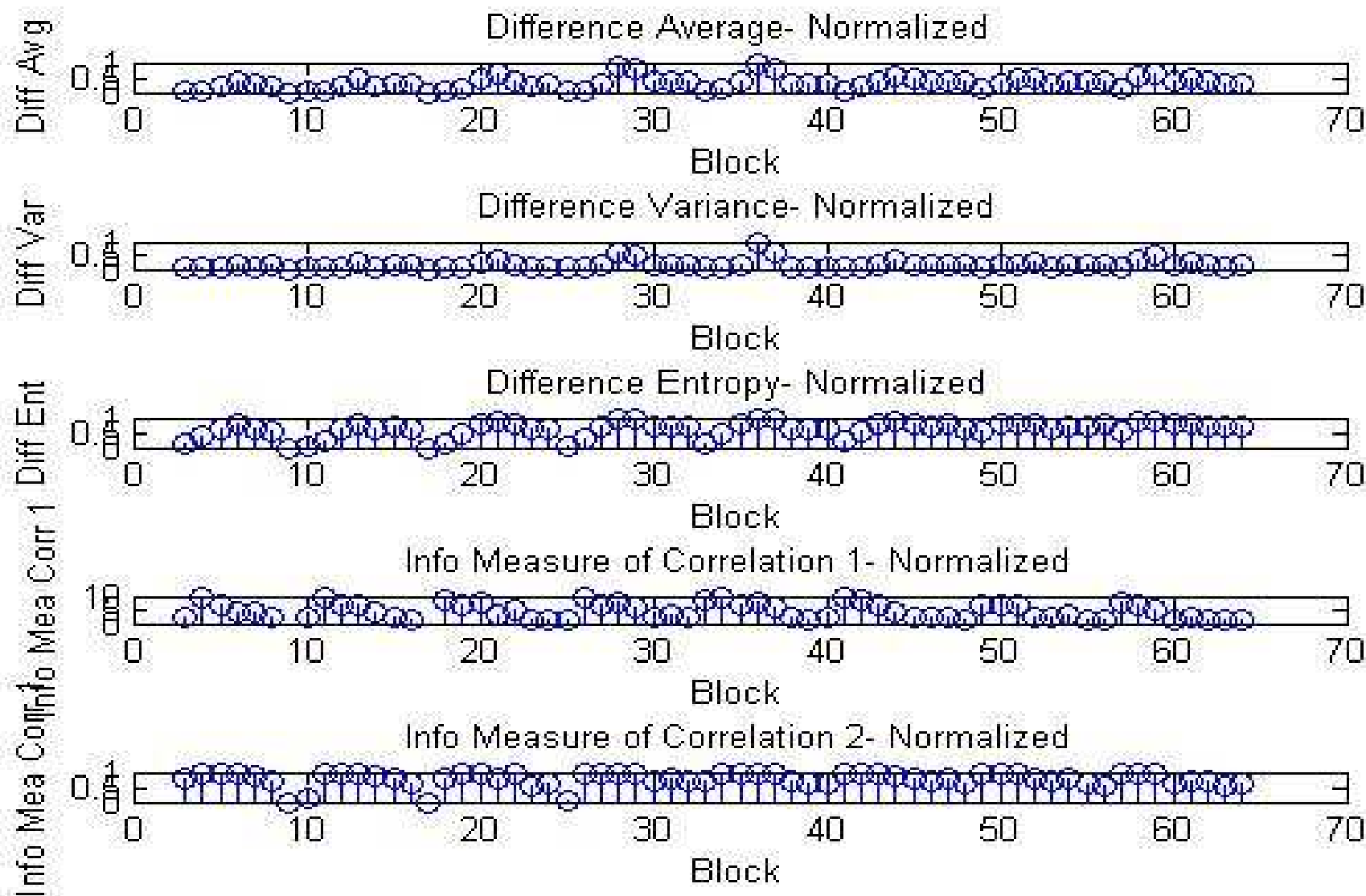
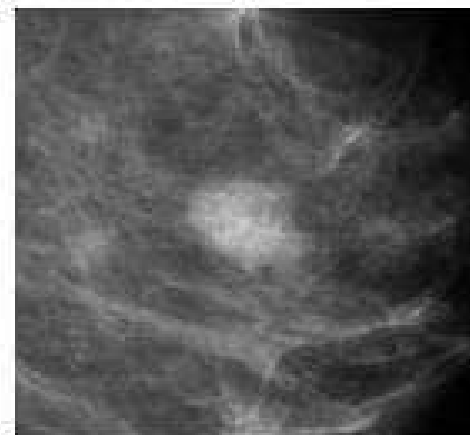


Image Segmentation- Region Growing

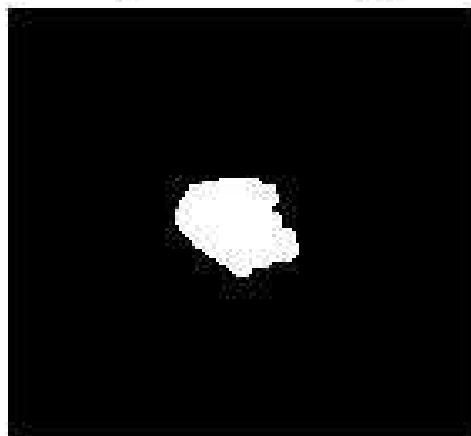
Original Image



Enhanced Image



Segmented Image



Estimated=29, Original=33

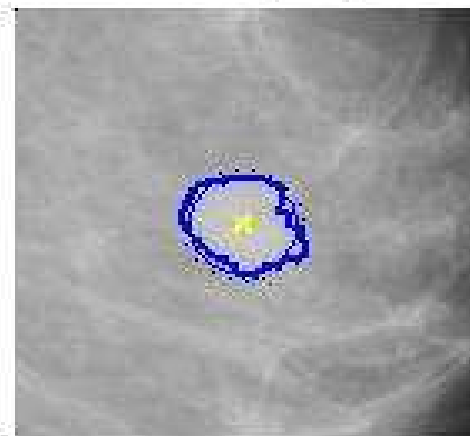
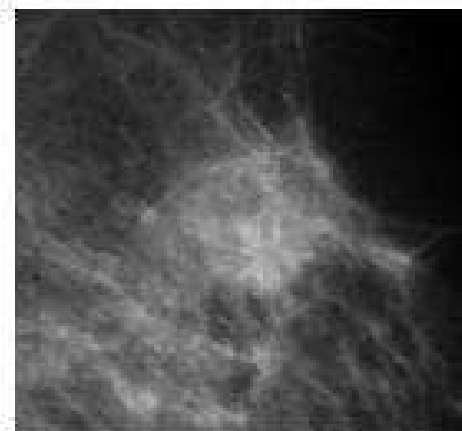


Image Segmentation- Contour Extraction

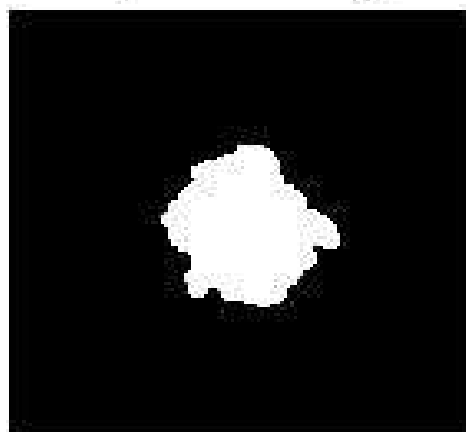
Original Image



Enhanced Image



Segmented Image



Extracted Contour

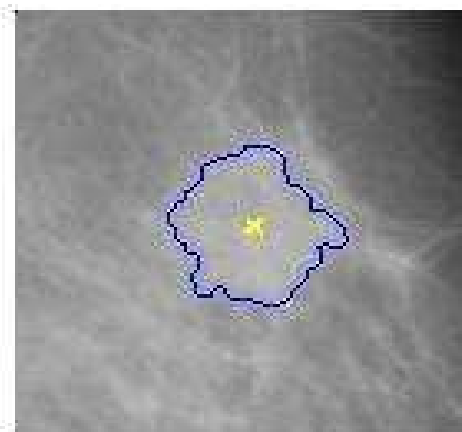
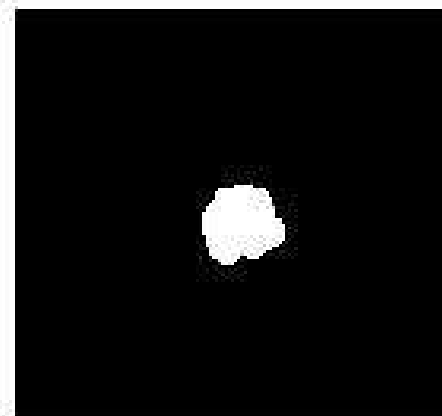


Image Segmentation- Mass Extraction

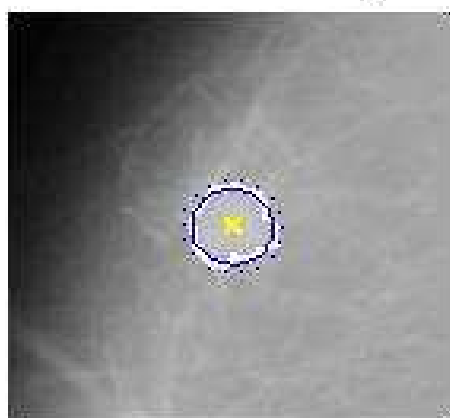
Original Image



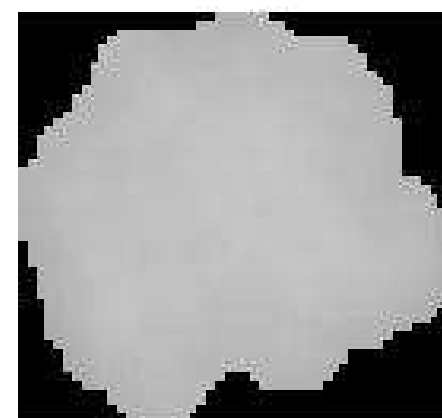
Segmented Image



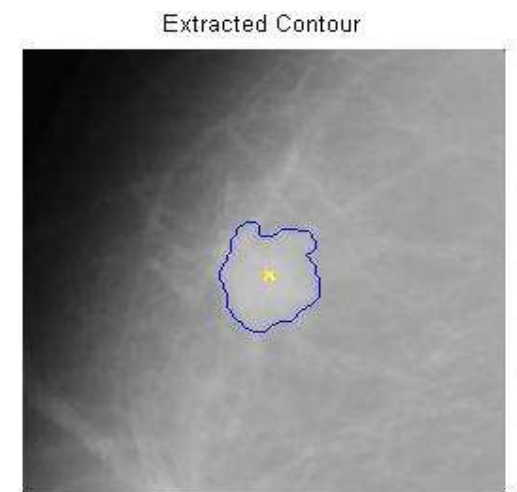
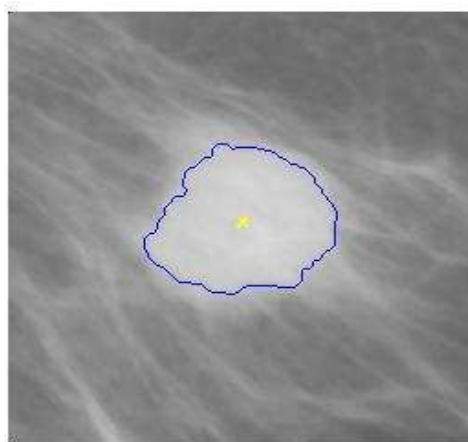
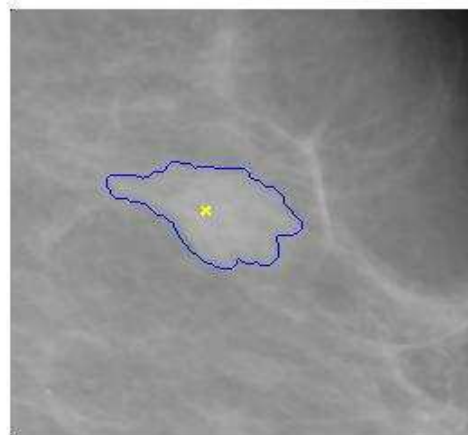
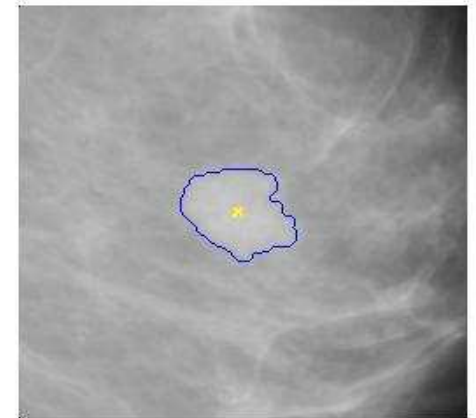
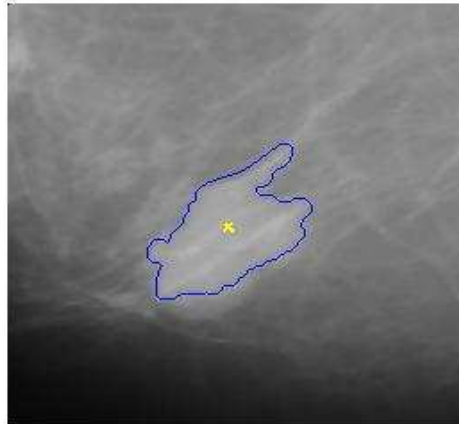
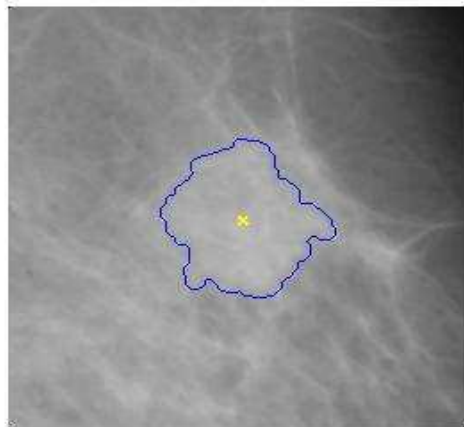
Estimated Mass Region



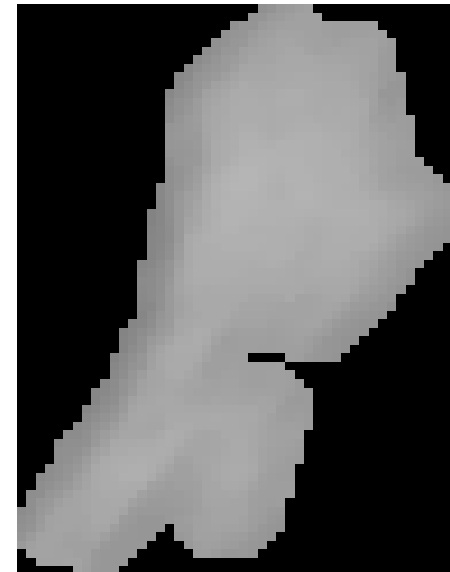
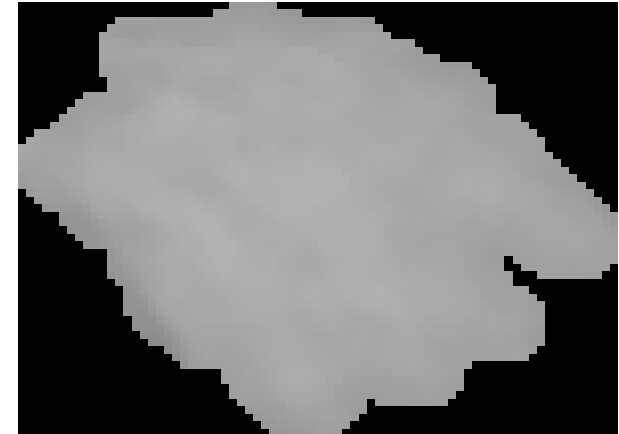
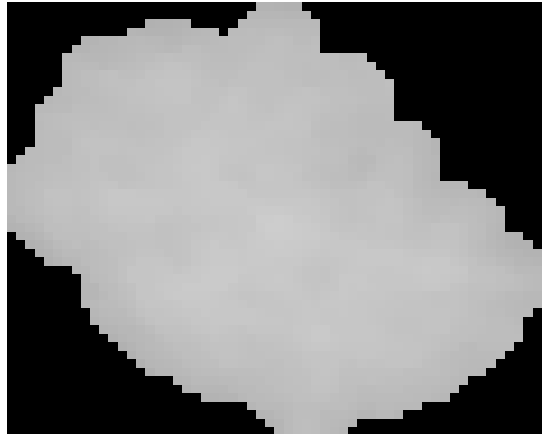
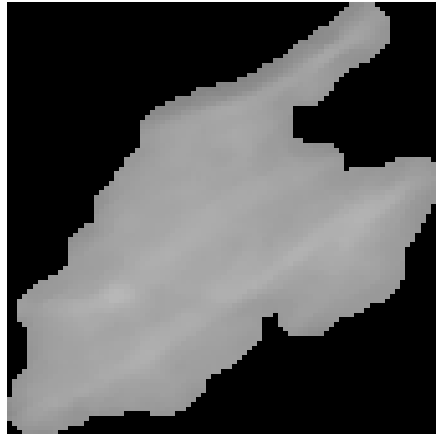
Extracted Mass



Contour Extraction Using Proposed Method



Mass Extraction Using Proposed Method



Observations

- **Image Enhancement**

- Since noise is also enhanced, noise is removed using median filtering
- For $k=4$, the image enhancement is satisfactory for this application.

$$I_{en}(i, j) = \left(\frac{I(i, j)}{I_{\max}} \right)^4 * I_{\max}$$

- **Image Segmentation**

- Block size 32x32 is found satisfactory
- Out of 13 Haralick texture features Sum Average is found very much significant to discriminate mass and non mass blocks.

$$Sum_Average = \sum_{k=2}^{N_g} k * p_{x+y}(k)$$

$$p_{x+y}(k) = \sum_{i=1}^{N_g} \sum_{j=1}^{N_g} p(i, j)$$

• N_g is distinct gray levels

$$i + j = k$$

Observations

- **Image Segmentation**

- Seed point is automatically selected that corresponds the maximum Sum Average feature value
- Segmented image is smoothed using some morphological operators like dilation, erosion, imopen and imclose.
- Extracted mass is approximated to a circle and compare it's radius to the original radius
- Extracted mass is used as an input to the classification stage

Segmentation Validation- Maple Leaf

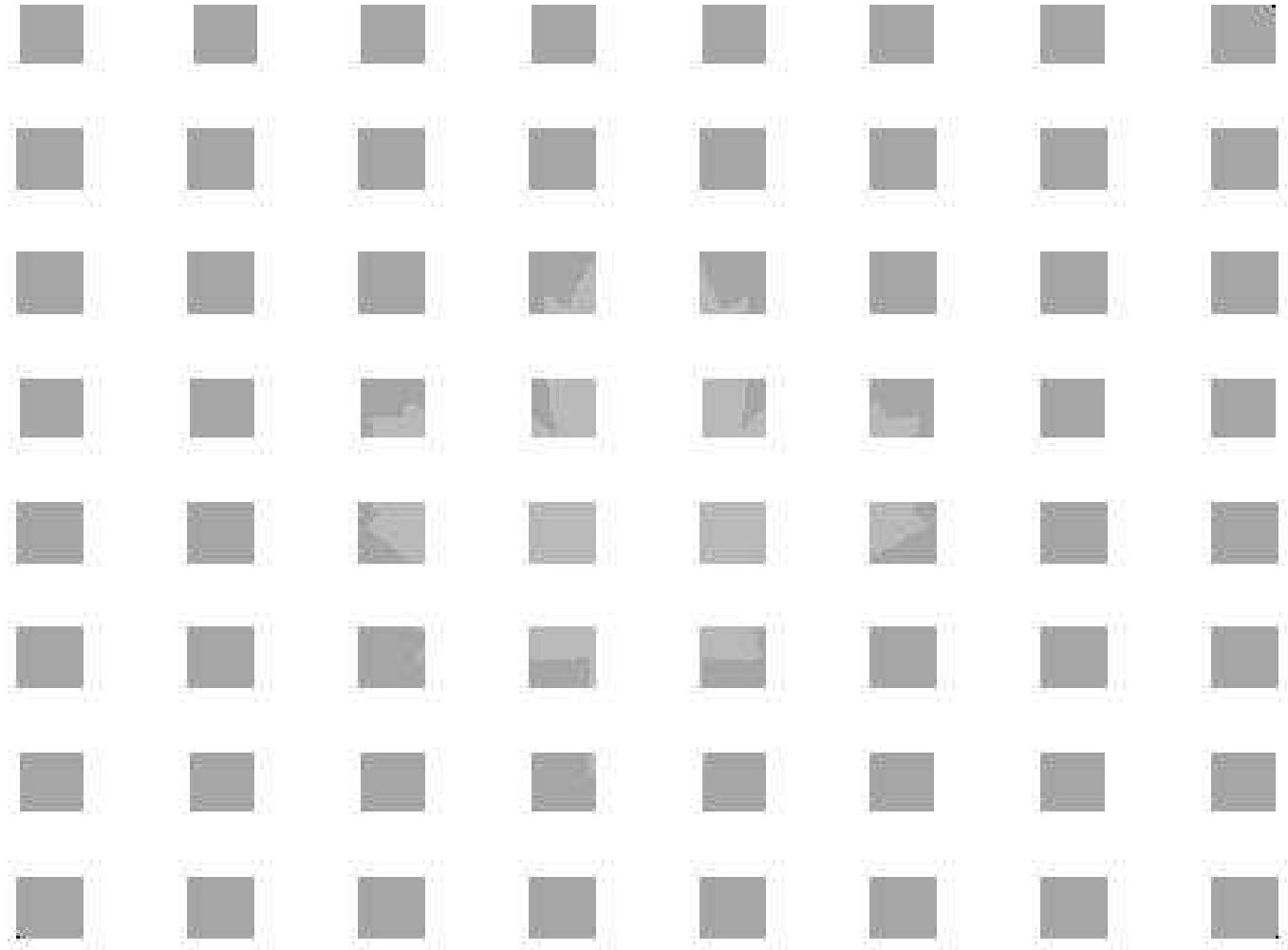
Original Image



Enhanced Image

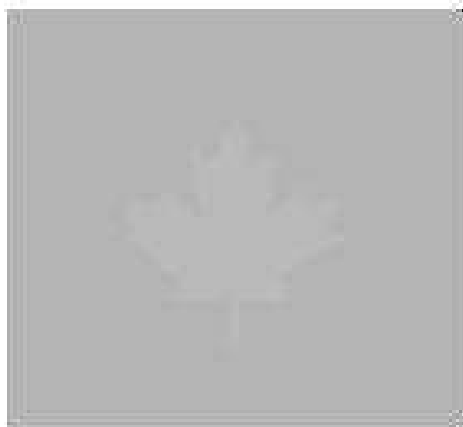


Segmentation Validation- Image Division



Segmentation Validation

Original Image



Enhanced Image



Segmented Image



Outlined Contour



Performance Evaluation

- **Efficiency:** Computational time is less as it starts from the seed point and grows iteratively to its neighborhood.
- **Adaptibility:** Evaluated on 82 images containing malignant and benign masses with different size, shape and contrast. The algorithm works properly in all cases
- **Robustness:** Evaluated with and without preliminary denoising steps. The two results are found to be comparable

Performance Evaluation

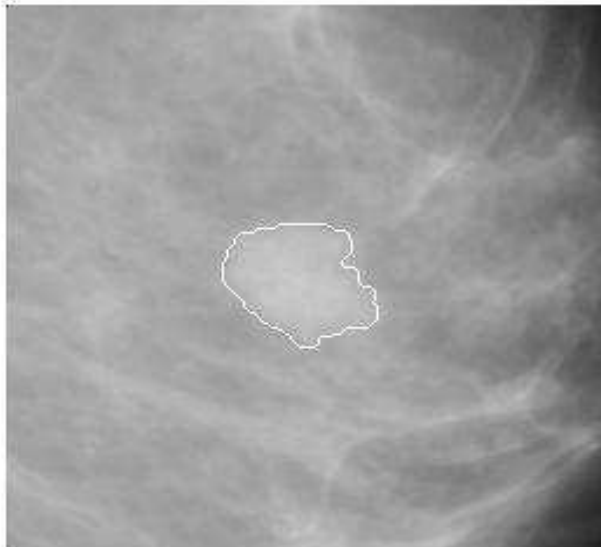
- Estimated Region (ER): Segmented Region
- Reference Region (RR): Circular area estimated by radiologist
- Area Difference (AD)= |area(RR) - area(ER)|
- True Positive (TP) regions: Intersection of ER and RR
- False Positive (FP) regions: The area not identified in RR
- False Negative (FN) regions: The area in RR not identified in ER
- Completeness (CM)
- Correctness (CR)

$$CM = \frac{TP}{TP + FN}$$

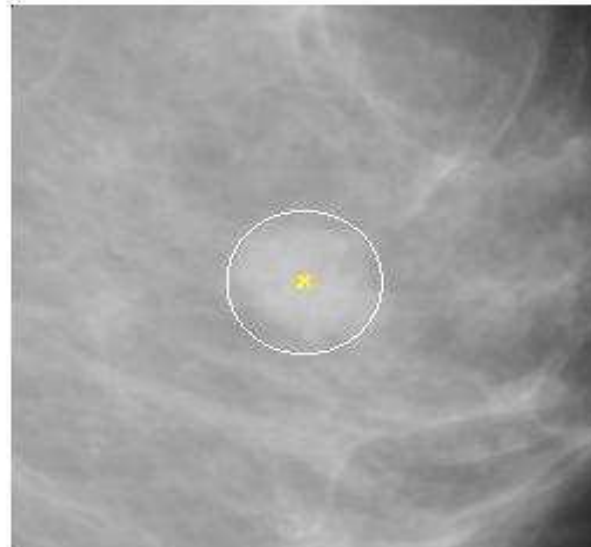
$$CR = \frac{TP}{TP + FP}$$

Performance Evaluation and Result Analysis

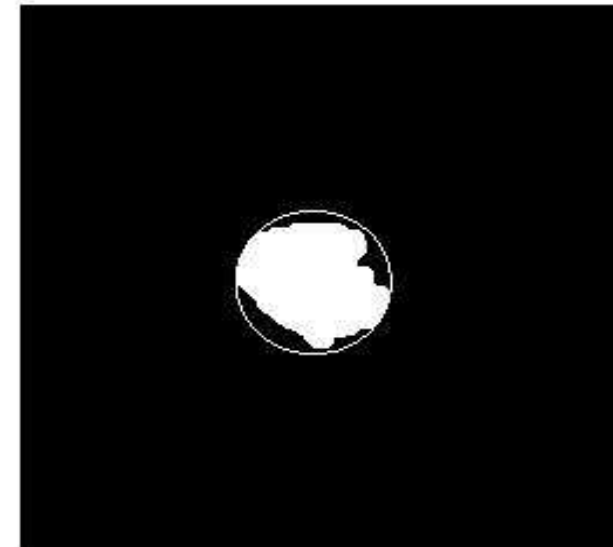
Estimated Mass Region



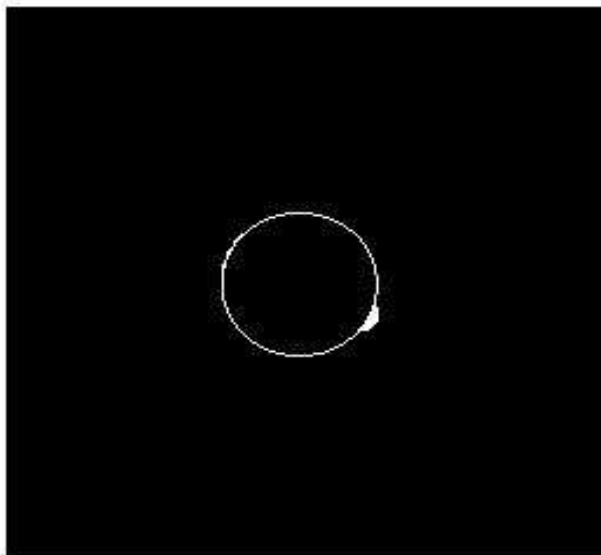
Reference Mass Region



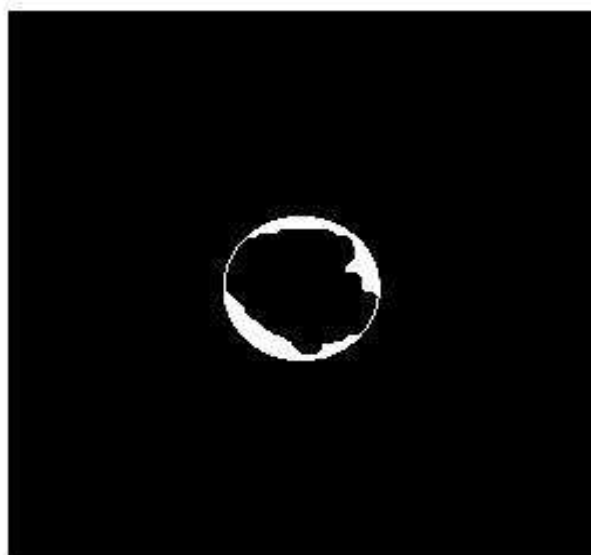
True Positive (TP) Region



False Positive (FP) Region

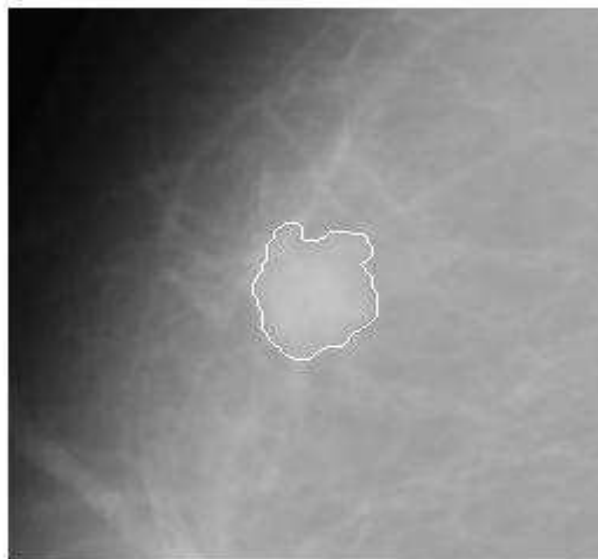


False Negative (FN) Region

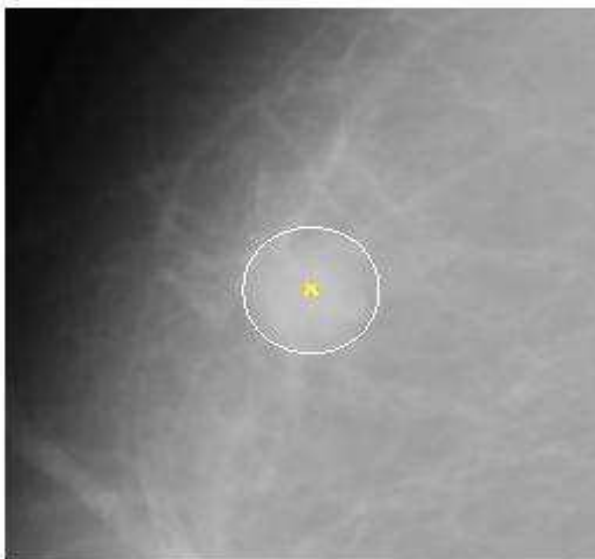


Performance Evaluation and Result Analysis

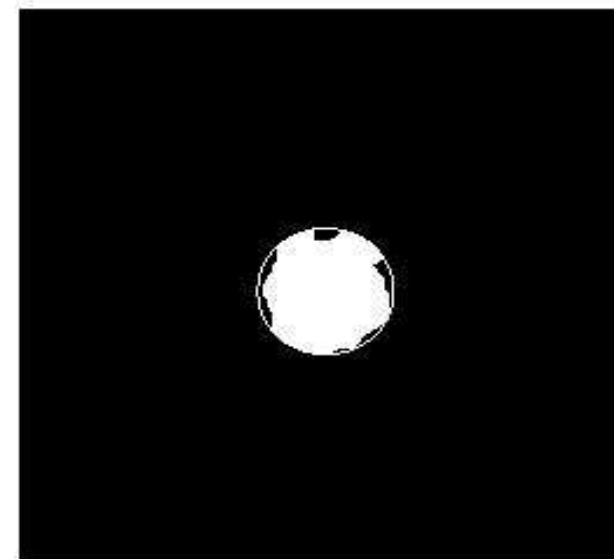
Estimated Mass Region



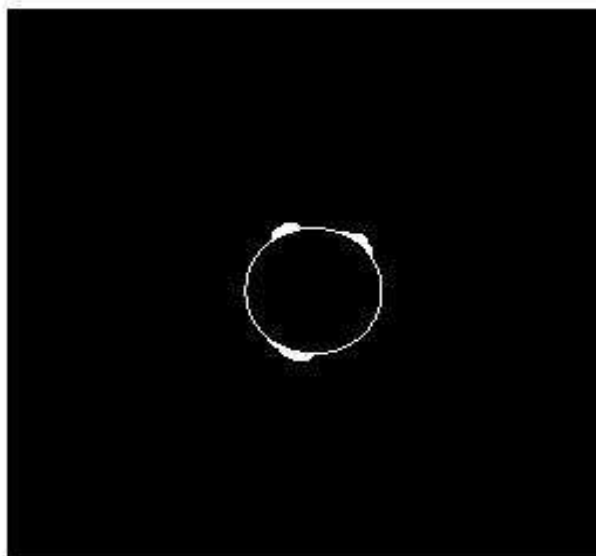
Reference Mass Region



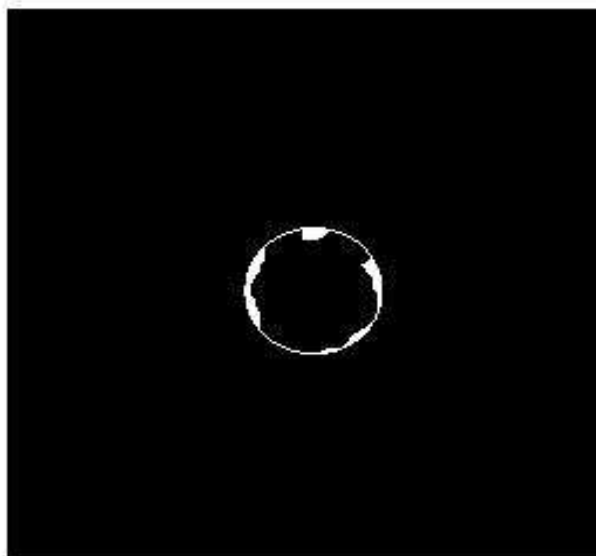
True Positive (TP) Region



False Positive (FP) Region



False Negative (FN) Region





Performance Evaluation- Result Analysis

Image	ER	RR	AD	TP	FP	FN	CM (%)	CR (%)
010_B	2714	3545	831	2665	49	880	75	98
012_B	4080	5172	1092	3485	595	1687	68	86
023_M	2541	2753	212	2403	138	350	87	95
028_M	6705	10053	3348	6705	0	3348	67	100
092_M	6017	5962	55	5486	531	476	92	91
Average							78	94

Sample Size: 82

Correct Segmentation (%)	Radiologist Sensitivity (%)	Incorrect Segmentation (%)
84.15% (69/82)	75%	15.85% (13/82)

Mass Classification- Artificial Neural Network (ANN)

- **Layers:** 3
- **Input Units:** Texture features (7)
- **Output Unit:** 1 (Benign=0, Malignant=1)
- **Hidden Units:** $(7+1)*2/3=5$
- **Total Weights:** $(7*5)+5=40$
- **Total Samples:** 69
- **Training Samples:** Benign (8), Malignant (8)- 25% (approx)
- **Testing Sample:** 53- 75% (approx)



Training Data Preparation

Feature Extraction From the Image

Load Image

Benign

Malignant

Features Calc

Save Features

Exit

Extracted Features

Mean : 0.757731854915619

Std. Deviation : 0.32649302482605

Smoothness : 0.0963292270898819

Entropy : 0.999977350234985

Skewness: -3.05705809593201

Kurtosis: 0.246905758976936

Uniformity: 0.140974879264832

Output : 1

Mass Classification- ANN Testing

Multilayer Perceptron Neural network Testing for Thresholding


Load Image

Classification

Output

1

Exit



Height

82

Width

100

Execution Time

0.031

Simulation Result- Mass Classification

- **Sample Size: 53 (Testing mass only)**
- **Benign: 31**
- **Malignant: 22**

Correct Classification (%)		Misclassification (%)		Radiologist Misclassification	
Benign	Malignant	Benign	Malignant	Benign	Malignant
83.87% (26/31)	90.91% (20/22)	16.63% (5/31)	9.09% (2/22)	65-90%	Not Available

Conclusions

- X-ray label is removed using global Otsu thresholding technique followed by connected component labeling
- Pectoral muscle is removed using automatic region growing
- ROI is extracted using peak analysis from the histogram of the breast tissue
- Image enhancement of the ROI is done using nonlinear operator
- Automated seed region growing is proposed for image segmentation.
- Automated seed selection is done using Haralick texture features. Sum Average is found the most discriminative features among 13 features.
- Segmented image is smoothed using mathematical morphology

Conclusions and Future Works

- Proposed segmentation technique is validated using artificial maple leaf image. It was blurred artificially and then segmented correctly using the proposed techniques.
- Performance of the proposed method is evaluated using two quantitative features Completeness (CM) and Correctness (CR).
- Correct segmentation is achieved 84.15% that is very much very promising compare to the radiologist's sensitivity 75%
- Artificial Neural Network is proposed for mass classification. Correct classification for benign is achieved 83.87% and for malignant 90.91%.
- Results are encouraging and have shown promise of our proposed system.
- **Future Works: Optimal features selection for classification of masses**



Thanks for your Patience.
Questions?

References

1. O.D Trier and A.K. Jain, "Goal-directed evaluation of binarization methods," IEEE Trans. on Pattern Recognition And Machine Intelligence, Vol. 17, no. 12, pp. 1191-1201, 1995.
2. W. Niblack, "An introduction to Digital Image Processing", Prentice Hall, Eaglewood Cliffs, NJ, pp. 115-116, 1986.
3. P.K. Sahoo, S. Soltani, A.K.C. Wong, "A Survey of thresholding techniques", Computer vision, Graphics and image Processing, Vol. 41, pp. 233-260, 1988
4. N. Otsu, "A Threshold Selection Method From Gray Level Histograms", IEEE Trans. On Systems, Man and Cybernetics, SMC-9, pp. 62-66, 1979
5. Y. Alginahi, "Computer Analysis of Composite Documents with Non-uniform Background", PhD Thesis, Electrical and Computer Engineering, University of Windsor, ON, Canada, 2004.
6. M.A. Sid-Ahmed, "Image Processing Theory, Algorithms and Architectures", McGraw-Hill, pp. 313-375, 1995.
7. R.C. Gonzalez, and R.E. Woods, "Digital Image Processing", Prentice-Hall, New Jersey, 2002
8. R. Koker and Y. Sari, "Neural Network Based Automatic Threshold Selection for an Industrial Vision System", Proc. Int. Conf. on Signal Processing, pp. 523-525, 2003
9. N. Papamarkos, "A Technique for Fuzzy Document Binarization", Procs. Of the ACM Symposium on 'Document Engineering, pp. 152-156, 2001.
10. Y. Alginahi, "Thresholding and character recognition in security documents with watermarked background", Proc. Int. Conf. on Digital Image Computing: Techniques and Applications (DICTA'08), pp. 220-225, 2008 .

References

11. Y. Alginahi, M.A. Sid-Ahmed and M. Ahmadi, “Local thresholding of composite documents using Multi-layer Perceptron Neural Network”, The 47-th IEEE International Midwest Symposium on Circuits and Systems, pp. I209- I212, 2004 .
12. Songtao Huang, Majid Ahmadi, M.A. Sid-Ahmed, “A hidden Markov model-based character extraction method”, pattern recognition, vol 41, pp. 2890-2900, 2008.
13. Adnan Khashman, Boran Sekeroglu, “ Document image binarization using a supervised neural network”, International Journal of Neural Systems, vol 18, No 5, pp. 405-418, 2008.
14. M. Sezgin and B. Sankur, “Survey over image thresholding techniques and quantitative performance evaluation”, Journal of Electronic Imaging, vol. 13, no. 1, pp. 146-165, 2004.
15. J. Kittler, J. Illingworth, “Minimum error thresholding”, Pattern Recognition, vol 19, pp. 41-47, 1986.
16. J.M.S. Prewitt, M.L. Mendelsohn, The analysis of cell images, Ann. New York Acad. Sci. 128 (1966) 1035–1053.
17. W. Doyle, Operation useful for similarity-invariant pattern recognition, J. Assoc. Comput. Mach. 9 (1962) 259–267.
18. J. Kittler, J. Illingworth, On threshold selection using illustering criteria, IEEE Syst. Man Cybern. 15 (1985) 652–655.
19. L. Hertz, R.W. Schafer, Multilevel thresholding using edge matching, CVGIP 44 (1988) 279–295.
20. A. Pikaz, A. Averbuch, Digital image thresholding based on topological stable state, Pattern Recognition 29 (1996) 829–843.

References

21. L.A. Fletcher, R. Kasturi, A robust algorithm for text string separation from mixed textgraphics images, *IEEE Trans. Pattern Anal. Mach. Intell.* 10 (6) (1988) 910–918.
22. M.K. Yanni, E. Horne, A new approach to dynamic thresholding, *EUSIPCO'94: 9th European Conference on Signal Processing*, vol. 1, Wiley, NY, 1994, pp. 34–44.
23. C.V. Jawahar, P.K. Biswas, A.K. Ray, Investigations on fuzzy thresholding based on fuzzy clustering, *Pattern Recognition* 30 (1997) 1605–1613.
24. E. Giuliano, O. Paitra, L. Stringa, Electronic character reading system, U.S. Patent 4, 047,15, 6 September, 1977.
25. K. Pal, A. Rosenfeld, Image enhancement and thresholding by optimization of fuzzy compactness, *Pattern Recognition Lett.* 7 (1988) 77–86.
26. A. Rosenfeld, The fuzzy geometry of image subsets, *Pattern Recognition Lett.* 2 (1984) 311–317.
27. W.H. Tsai, Moment-preserving thresholding: a new approach, *Graph. Models Image Process.* 19 (1985) 377–393.
28. S.C. Cheng, W.H. Tsai, A neural network approach of the moment preserving technique and its application to thresholding, *IEEE Trans. Comput.* C-42 (1993) 501–507.
29. E.J. Delp, O.R. Mitchell, Moment-preserving quantization, *IEEE Trans. Commun.* 39 (1991) 1549–1558.
30. W.A. Yasnoff, J.K. Mui, J.W. Bacus, Error measures for scene segmentation, *Pattern Recognition* 9 (1977) 217–231.
31. M.D. Levine, A.M. Nazif, Dynamic measurement of computer generated image segmentations, *IEEE Trans. Pattern Anal. Mach. Intell.* 7 (1985) 155–164.
32. Y.J. Zhang, A survey on evaluation methods for image segmentation, *Pattern Recognition* 29 (1996) 1335–1346.

References

33. S.H. Nam, J.Y. Choi, A method of image enhancement and fractal dimension for detection of microcalcifications in mammogram, in: Proceedings of the 20th Annual International Conference of the IEEE Engineering in Medicine and Biology Society 20, vol. 2, 1998, pp. 1009–1012.
34. M. Wilson, R. Hargrave, S. Mitra, Y.Y. Shieh, G.H. Roberson, Automated detection of microcalcifications in mammograms through application of image pixel remapping and statistical filter, in: Proceedings of the IEEE Symposium on Computer-based Medical Systems, 1998, pp. 270–274.
35. K. Wongsritong, K. Kittayarusiriwat, F. Cheevasuvit, K. Dejhan, A. Somboonkaew, Contrast enhancement using multipeak histogram equalization with brightness preserving, in: IEEE Asia-Pacific Conference on Circuits and Systems—Proceedings, 1998, pp. 455–458.
36. H.D. Cheng, X.J. Shi, A simple and effective histogram equalization approach to image enhancement, *Digital Signal Process.* 14 (2) (2004) 158–170.
37. J.K. Kim, J.M. Park, K.S. Song, H.W. Park, Adaptive mammographic image enhancement using first derivative and local statistics, *IEEE Trans. Med. Imaging* 16 (5) (1997) 495–502.
38. D. Braccialarghw, G.H. Kaufmann, Contrast enhancement of mammographic features: a comparison of four methods, *Opt. Eng.* 35 (1) (1996) 76–80.

References

39. V. Gimenez, D. Manrique, J. Rios, A. Vilarrasa, Iterative method for automatic detection of masses in digital mammograms for computeraided diagnosis, in: Proceedings of SPIE—The International Society for Optical Engineering 3661, vol. II, 1999, pp. 1086–1093.
40. T. Matsubara, H. Fujita, S. Kasai, M. Goto, Y. Tani, T. Hara, T. Endo, Development of new schemes for detection and analysis of mammographic masses, Intel. Inform. Systems (1997) 63–66.
41. L.H. Li, W. Qian, L.P. Clarke, R.A. Clark, J. Thomas, Improving mass detection by adaptive and multi-scale processing in digitized mammograms, in: Proceedings of SPIE—The International Society for Optical Engineering 3661, vol. 1, 1999, pp. 490–498.
42. H.D. Li, M. Kallergi, L.P. Clarke, V.K. Jain, R.A. Clark, Markov random field for tumor detection in digital mammography, IEEE Trans. Med. Imaging 14 (3) (1995) 565–576.
43. M. Abdel-Mottaleb, C.S. Carman, C.R. Hill, S. Vafai, Locating the boundary between breast skin edge and the background in digitized mammograms, in: K. Doi, M.L. Giger, R.M. Nishikawa, R.A. Schmidt (Eds.), Digital Mammography, Elsevier, Amsterdam, 1996, pp. 467–470.
44. M. Kallergi, K. Woods, L.P. Clarke, W. Qian, R.A. Clark, Image segmentation in digital mammography: comparison of local thresholding and region growing algorithms, Comput. Med. Imaging Graph. 16 (5) (1992) 231–323.

References

45. R.M. Rangayyan, L. Shen, Y. Shen, J.E.L. Desautels, H. Bryant, T.J. Terry, N. Horeczko, M.S. Rose, Improvement of sensitivity of breast cancer diagnosis with adaptive neighborhood contrast enhancement of mammograms, *IEEE Trans. Inform. Technol. BioMed.* 1 (3) (1997) 161–170.
46. Y.J. Lee, J.M. Park, H.W. Park, Mammographic mass detection by adaptive thresholding and region growing, *Int. J. Imaging Systems Technol.* 11 (5) (2000) 340–346.
47. S.A. Hojjatoleslami, J. Kittler, Region growing: a new approach, *IEEE Trans. Image Process.* 7 (7) (1998) 1079–1084.
48. N. Petrick, H.P. Chan, B. Sahiner, D. Wei, An adaptive density weighted contrast enhancement filter for mammographic breast mass detection, *IEEE Trans. Med. Imaging* 15 (1) (1996) 59–67.
49. J.L. Viton, M. Rasigni, G. Rasigni, A. Liebaria, Method for characterizing masses in digital mammograms, *Opt. Eng.* 35 (12) (1996) 3453–3459.
50. N. Petrick, H.P. Chan, B. Sahiner, D. Wei, M.A. Helvie, M.M. Goodsitt, D.D. Adler, Automated detection of breast masses on digital mammograms using adaptive density-weighted contrast enhancement filtering, *Proceedings of SPIE—The International Society for Optical Engineering*, vol. 2434, 1995, pp. 590–597.
51. N. Petrick, H.P. Chan, D. Wei, B. Sahiner, M.A. Helvie, D.D. Adler, Automated detection of breast masses on mammograms using adaptive contrast enhancement and texture classification, *Med. Phys.* 23 (10) (1996) 1685–1696.

References

52. H. Kobatake, M. Murakami, H. Takeo, S. Nawano, Computerized detection of malignant tumors on digital mammograms, *IEEE Trans. Med. Imaging* 18 (5) (1999) 369–378.
53. J.F. Canny, A computational approach to edge detection, *IEEE Trans. Pattern Anal. Mach. Intel.* 8 (6) (1986) 679–698.
54. S.M. Lai, X. Li, W.F. Bischof, On techniques for detecting circumscribed masses in mammograms, *IEEE Trans. Med. Imaging* 18 (4) (1989) 377–386.
55. S. Morrison, L.M. Linnett, A model based approach to object detection in digital mammography, in: *Proceedings of the IEEE International Conference on Image Processing*, vol. 2, Kobe, Japan, 1999, pp. 182–186.
56. S.L. Ng, W.F. Bischof, Automated detection and classification of breast tumors, *Comput. Biomed. Res.* 25 (1992) 218–237.
57. F.N. Che, M.C. Fairhurst, C.P. Wells, M. Hanson, Evaluation of a two-stage model for detection of abnormalities in digital mammograms, in: *Proceedings of the 1996 IEE Colloquium on Digital Mammography*, No. 072, London, UK, 1996.
58. Y. Hatanaka, T. Hara, H. Fujita, S. Kasai, T. Endo, T. Iwase, Development of an automated method for detecting mammographic masses with a partial loss of region, *IEEE Trans. Med. Imaging* 20 (12) (2001) 1209–1214.
59. G.D. Tourassi, Rene Vargas-Voracek, Computer-assisted detection of mammographic masses: a template matching scheme based on mutual information, *Med. Phys.* 30 (2003) 2123–2130.

References

60. B. Zheng, Y.H. Chang, D. Gur, Computerized detection of masses from digitized mammograms: comparison of single image segmentation and bilateral-image subtraction, *Assoc. Univ. Radiologists* 2 (12) (1995) 1056–1061.
61. F.F. Ying, M.L. Giger, C.J. Vyborny, K. Doi, R.A. Schmidt, Comparison of bilateral-image subtraction and single-image processing techniques in the computerized detection of mammographic masses, *Invest. Radiol.* (1993) 473–481.
62. M.L. Giger, F.F. Yin, K. Doi, Y. Wu, C.J. Vyborny, R.A. Schmidt, Z. Huo, Computerized detection and characterization of mass lesions in digital mammography, 1992 IEEE International Conference on Systems, Man and Cybernetics, vol. 2, Chicago, IL, 1992, pp. 1370–1372.
63. F.F. Yin, M.L. Giger, K. Doi, C.E. Metz, C.J. Vyborny, R.A. Schmidt, Computerized detection of masses in digital mammograms: analysis of bilateral subtraction images, *Med. Phys.* 18 (5) (1991) 955–963.
64. T.K. Lau, W.F. Bischof, Automated detection of breast tumors using the asymmetry approach, *Comput. Biomed. Res.* 24 (1991) 273–295.
65. A.J. Mendez, P.G. Tahoces, M.J. Lado, M. Souto, J.J. Vidal, Computer-aided diagnosis: automatic detection of malignant masses in digitized mammograms, *Med. Phys.* 25 (6) (1998) 957–964.
66. A. Hadjarian, J. Bala, S.A. Gutta, S. Trachiotis, P. Pachowicz, The fusion of supervised and unsupervised techniques for segmentation of abnormal regions, in: N. Karssemeijer, M. Thijssen, J. Hendriks, L. Erning (Eds.), *Digital Mammography*, Kluwer, Amsterdam, 1998, pp. 299–302.

References

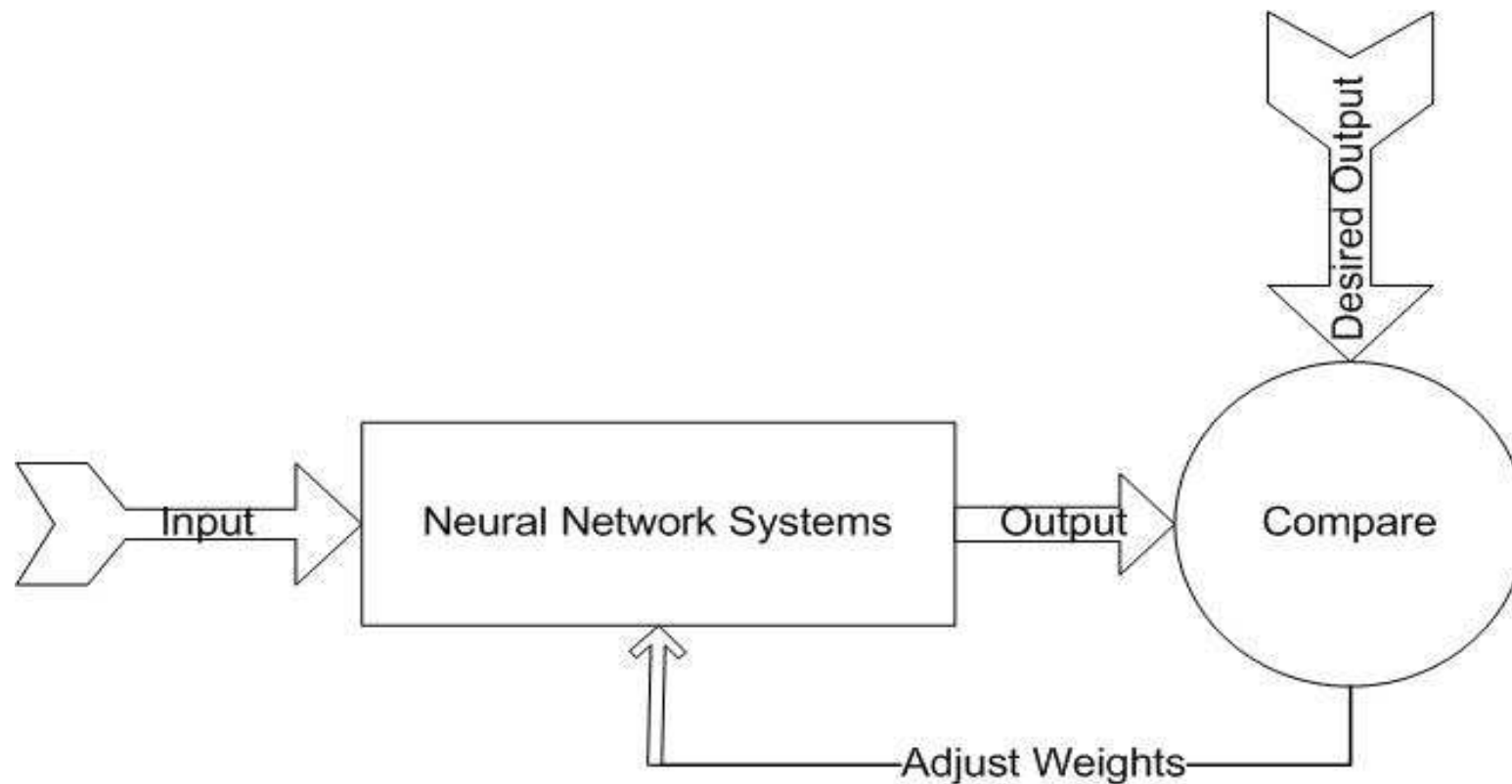
67. M. Sameti, R.K. Ward, A fuzzy segmentation algorithm for mammogram partitioning, in: K. Doi, M.L. Giger, R.M. Nishikawa, R.A. Schmidt (Eds.), *Digital Mammography*, Elsevier, Amsterdam, 1996, pp. 471–474.
68. M. Sameti, R.K. Ward, B. Palcic, J. Morgan-Parkes, Texture feature extraction for tumor detection in mammographic images, 1997 IEEE Pacific Rim Conference on Comm., Computers and Signal Processing, 1997, pp. 831–834.
69. M. Sameti, R.K. Ward, J. Morgan-Parkes, B. Palcic, A method for detection of malignant masses in digitized mammograms using a fuzzy segmentation algorithm, in: *Proceedings of the 19th International Conference IEEE/MBS*, 2000, pp. 513–516.
70. D. Guliato, R.M. Rangayyan, W.A. Carnielli, J.A. Zuffo, J.E.L. Desautels, Segmentation of breast tumors in mammograms by fuzzy region growing, *The IEEE Proceedings of the 20th Annual International Conference on Engineering in Medicine and Biology Society*, vol. 2, 1998, pp. 1002–1005.
71. D. Guliato, R.M. Rangayyan, W.A. Carnielli, J.A. Zuffo, J.E.L. Desautels, Detection of breast tumor boundaries using iso-intensity contours and dynamic thresholding, in: *Proceedings of the Fourth International Workshop Digital Mammography*, The Netherlands, 1998, pp. 253–260.
72. P. Undrill, R. Gupta, S. Henry, M. Dowing, Texture analysis and boundary refinement to outline mammography masses, *Proceedings of the 1996 IEE colloquium on Digital mammography*, 1996, pp. 51-56

References

73. N. Petrick, H.P. Chan, B. Sahiner, M.A. Helvie, Combined adaptive enhancement and region growing segmentation of breast masses on digitized mammograms, *Med. Phys.* 26 (1999) 1642-1654.
74. R.O. Duda, P.E. Hatt, D.G. Stork, *Pattern classification*, second ed. Wiley, New York, 2001
75. P.A. Lachenbruch, *Discriminant analysis*, Hafner, New York, 1975
76. Christoyianni, E. Darmatas, G. Kokkinakis, Fast detection of masses in computer- aided mammography, *IEEE Signal Processing Mag.* 17 (1), 2000, pp. 54-64.
77. B. Sahiner, H.P. Chan, M.A. Helvie, M.M. Goodsitt, Computerized classification of benign and malignant masses on digitized mammograms: a study of robustness, *Acad. Radiology.* 7, 2000, 1077-1084
78. G.M. Brake, N. Karssemeijer, J.H.C.L. Hendriks, An automatic method to discriminate malignant masses from normal tissue in digital mammograms, *Phys. Med. Biol.* 45 (10), 2000, 2843-2857
79. R.M. Haralick, K. Shanmugam, I.K. Denstein, Textural Features for Image Classification, *IEEE transactions on systems, man and cybernatics*, vol. 3(6), 610-621, 1973.
80. R.E. Bird, Professional quality assurance for mammography screening programs, *Radiology*, 175 587, 1990.
81. H.D. Cheng, X.J. Shi, R. Min, L.M. Hu, X.P. Cai, H.N. Du, Approaches for automated detection and classification of masses in mammograms, *Pattern recognition*, 39, 646-668, 2006

How does ANN work?

- ANNs are adjusted or trained so that a particular input leads to a specific desired or target output



Multi-Layer Perceptron (MLP)

- Most common NN model
- Uses supervised training methods to train the NN

